AD-A058 304 SCIENCE APPLICATIONS INC MCLEAN VA F/G 18/3
EXPERIMENTAL STUDIES OF SOIL THERMAL IRRADIATION. VOLUME III. D--ETC(U)
APR 77 A HOUGHTON, T M KNASEL DNA001-75-C-0209
UNCLASSIFIED SAI-78-540-WA-VOL-3 DNA-4484F-3 NL

1 OF 1
AD
A058304

END
DATE
FILMED
10-78
DDC

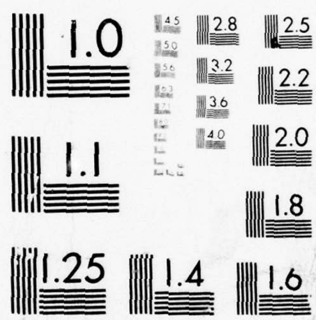
1.0
1.1
1.25
1.4
1.6
1.8
2.0
2.2
2.5
2.8
3.2
3.6
4.0
4.5
5.0
5.6

DNA 4484F-3

EXPERIMENTAL STUDIES OF SOIL THERMAL IRRADIATION

Volume III – Design of Flux Diversion Equipment for Soil Irradiation Testing

Science Applications, Inc.
8400 Westpark Drive
McLean, Virginia 22101

15 April 1977

Final Report for Period 1 January 1976–1 March 1977

CONTRACT No. DNA 001-75-C-0209

APPROVED FOR PUBLIC RELEASE;
DISTRIBUTION UNLIMITED.

THIS WORK SPONSORED BY THE DEFENSE NUCLEAR AGENCY UNDER RDT&E RMSS CODE B344077464 Y99QAXSA00205 H2590D.

Prepared for
Director
DEFENSE NUCLEAR AGENCY
Washington, D. C. 20305

(18) DNA, SBIE (19) 4484F-3, AD-E300 289

UNCLASSIFIED

SECURITY CLASSIFICATION OF THIS PAGE (*When Data Entered*)

REPORT DOCUMENTATION PAGE

READ INSTRUCTIONS BEFORE COMPLETING FORM

1. REPORT NUMBER: DNA 4484F-3
2. GOVT ACCESSION NO.:
3. RECIPIENT'S CATALOG NUMBER: (9)
4. TITLE (*and Subtitle*): (6) EXPERIMENTAL STUDIES OF SOIL THERMAL IRRADIATION. Volume III. Design of Flux Diversion Equipment for Soil Irradiation Testing.
5. TYPE OF REPORT & PERIOD COVERED: Final Report, ~~for Period~~ 1 Jan 76—1 Mar 77,
6. PERFORMING ORG. REPORT NUMBER: (14) SAI-78-540-WA-VOL-3
7. AUTHOR(s): (10) A. Houghton, T. M. Knasel
8. CONTRACT OR GRANT NUMBER(s): (15) DNA 001-75-C-0209
9. PERFORMING ORGANIZATION NAME AND ADDRESS: Science Applications, Inc., 8400 Westpark Drive, McLean, Virginia 22101
10. PROGRAM ELEMENT, PROJECT, TASK AREA & WORK UNIT NUMBERS: NWED Subtask Y99QAXSA002-05 (16) (17) A002
11. CONTROLLING OFFICE NAME AND ADDRESS: Director, Defense Nuclear Agency, Washington, D.C. 20305
12. REPORT DATE: (11) 15 Apr 1977
13. NUMBER OF PAGES: 48 (12) 48p.
14. MONITORING AGENCY NAME & ADDRESS (*if different from Controlling Office*):
15. SECURITY CLASS (*of this report*): UNCLASSIFIED
15a. DECLASSIFICATION/DOWNGRADING SCHEDULE:

16. DISTRIBUTION STATEMENT (*of this Report*)

Approved for public release; distribution unlimited.

17. DISTRIBUTION STATEMENT (*of the abstract entered in Block 20, if different from Report*)

18. SUPPLEMENTARY NOTES

This work sponsored by the Defense Nuclear Agency under RDT&E RMSS Code B344077464 Y99QAXSA00205 ~~H2590D~~.

19. KEY WORDS (*Continue on reverse side if necessary and identify by block number*)

Soil Thermal Irradiation
Thermal Layer Development
Precursor Effect
Non-Ideal Blast Wave
Nuclear Burst Simulation
Solar Furnace

20. ABSTRACT (*Continue on reverse side if necessary and identify by block number*)

The total report describes three experimental activities in thermal layer experimental development. Volume I analyzes soil irradiation tests performed under previous contracts. Thorough cross comparison of over twenty soil types revealed that these could be apportioned into seven key categories of soil response behavior. Volume II reports on an innovative thermochemical pulse generator development program. Volume III contains descriptions of design and experimental work directed toward the use of a flux redirector for a large → over

DD FORM 1473, 1 JAN 73 — EDITION OF 1 NOV 65 IS OBSOLETE

UNCLASSIFIED

SECURITY CLASSIFICATION OF THIS PAGE (*When Data Entered*)

408404 78 06 16 031

20. ABSTRACT (Continued)

solar furnace. Successful completion of this design allows testing of soils at above 300 cal/cm^2 sec.

(cont on p

sq cm

Table of Contents

List of Illustrations

Section 1

OBJECTIVES AND REQUIREMENTS

(cont AP1423A)

1.1 PROGRAM OBJECTIVES

An The objective of the tasks reported in this volume is an investigation was made of the feasibility of an ~~extention of~~ extending the solar furnace source soil blow-off tests (reported in Volume I) to higher flux levels. Previous work had identified the CNRS solar furnace at Odeillo-Font Romeu, France, as the unique radiant energy source (Reference 1). Accomplishment of the tests would require:

a) Design of an optical configuration to direct the solar furnace flux onto horizontal soil samples (necessitating a 90 deg redirection); Fullscale modeling, and testing of the optical equipment.

b) Construction of the critical optical and mechanical components and testing in the actual solar furnace environment.

c) Design and construct an instrumentation package to measure irradiation and sample response,

d) Preparation and characterization of samples, and

e) Conducting soil exposure tests and analyzing

f) Analysis of test data.

It was requested that in order to indicate feasibility of design and modeling of the critical optical components would be accomplished. A decision point is reached if this is shown to be technically feasible. Consequently, this report is limited to the effort related to the design of the critical optical components. Although some design effort was expended on the shutter and instrument package design, it was not extensive enough to produce more than an indication that the required instruments could be designed to meet the experimental constraints.

1.2 BASIC REQUIREMENTS

The basic requirements for the critical components are

a) Turn the CNRS furnace flux by 90^o

b) Contain soil blow-off in a flow tube above the soil surface

c) Withstand the severe environment of the test sequence

d) Allow for the use of auxiliary instruments and equipment

e) Be of small physical size and minimal cost.

The basic requirements must be related to the physical characteristics of the CNRS solar furnace, the ranges of flux and fluence required at the soil surface and type and quantities of data needed for characterization of soil blow-off phenomena.

a. <u>CNRS Solar Furance</u>

The optical systems of CNRS solar furnace is composed of a field of 63 tracking heliostats, each of which has an area of 45 M^2, and a faceted parabolic concentrator 54 M wide and 40 M high with a focal length of 18 M. More than one megawatt of thermal power is delivered to the focus. The peak flux at the focus is about 1600 w/cm^2 sec and the 800 w/cm^2 sec contour is approximately a 10 cm radius from the center of the focal spot.

The furnace has a large relative aperature (approximately f/0.35, although the parabolic concentrator does not have a uniform diameter). Energy arrives at the focus with an angular spread of 150^o in the horizontal and 114^o in the vertical. Figure 1-1 shows the geometry of the furnace. Figure 1-2 shows the flux contours at the focal plane. Further description of the CNRS furnace is given in Reference 2, Section 4.

Attenuation can be accomplished by reducing the number of heliostats used to direct the solar energy to the parabola.

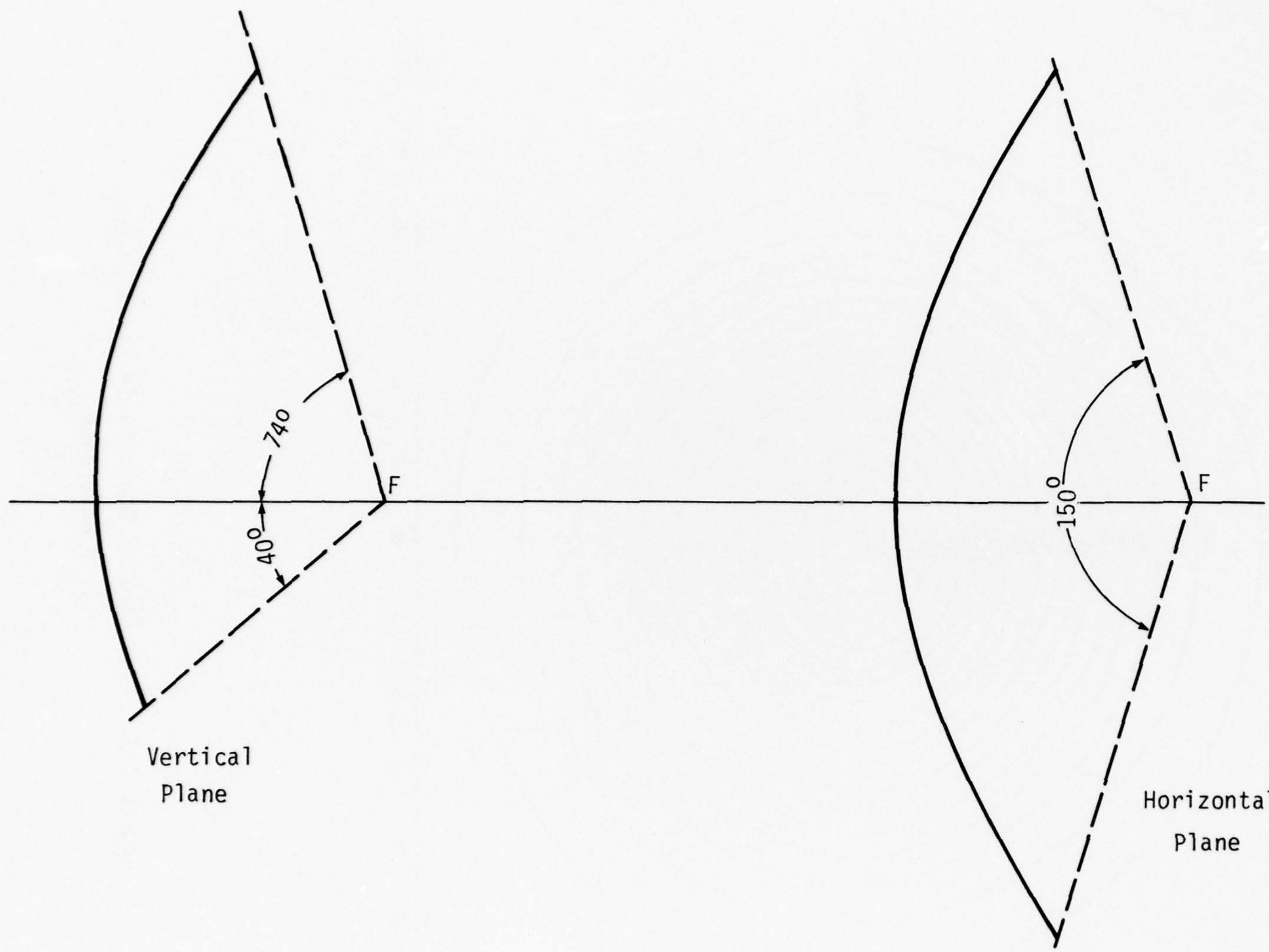

Figure 1-1. CNRS Beam Geometry

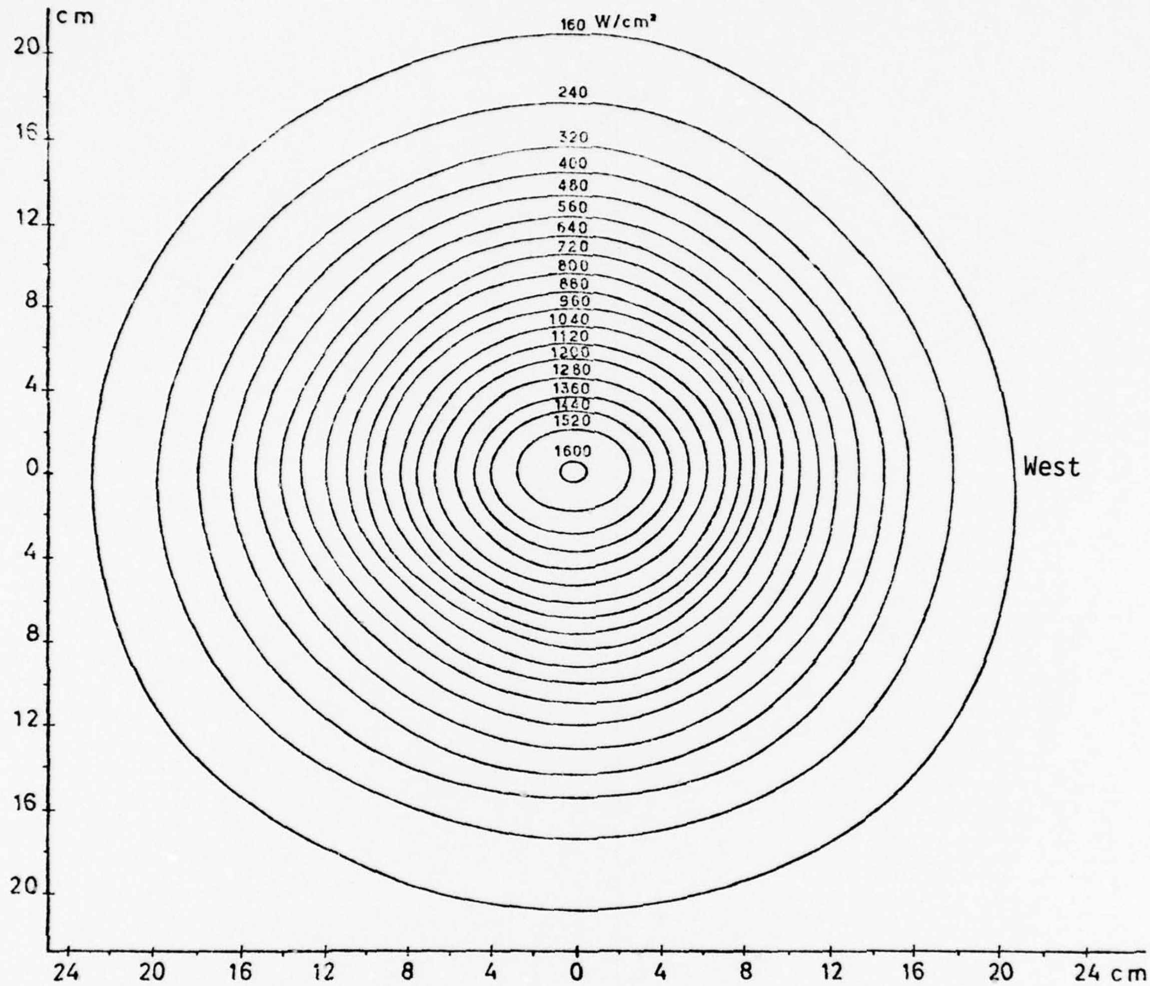

Figure 1-2. Flux Density Contours in Focal Plane
(from Reference 1)

b. Flux and Fluence Design Requirements

For the initial design, peak flux and peak fluence on the horizontal soil surface were determined as follows: peak flux within 60% of furnace peak flux of 450 cal/cm^2 sec and a fluence up to 1000 cal/cm^2.

c. Blow-Off Containment

The irradiated area will be relatively small, probably in the range from 200 to 500 cm^2. To retain the one dimensional nature of the actual thermal layer development, the column of air over the sample must be contained to avoid horizontal expansion. The height of the column must be sufficient to permit measurements at elevation of interest and it must not be impeded or modified in its vertical expansion.

These requirements suggest a smooth walled optically reflecting containment tube having an open top and a height of approximately one meter.

d. Data Requirements

The minimum data required for each test are as follows:

- Sample identification and description including chemical and geological classification, source location, distribution of grain size, H_2O content and mass.
- Post-exposure sample data including mass, surface effects and changes in chemical composition.
- Radiant input data. These may be estimated from measurements made under essentially identical conditions without a soil sample.
- Temperature of the soil sample just below its surface.
- Samples of blow-off particles.
- Temperature of the air column at several selected elevations.

Additional data that would be useful in interpretation of the results include:

- High speed photography of the steam, smoke and particulate blow-off from the sample surface.

- Albedo of the soil sample surface prior to and during irradiation.
- Reradiation from soil surface.

The first four of the foregoing data requirements do not impose any design constraints on the critical optical components. The others imply the presence of instruments in the containment tube or openings in the tube for data acquisition.

e. Number of Tests

To ensure that data represent a realistic range of yields, height of burst and ground ranges, it is estimated that eleven successful tests will be required for each soil type.

For planning purposes a series of tests including 10 soil types (similar to the seven basic bare soil types studies in previous work, plus three samples with vegetation included) was assumed). Thus, a minimum of 110 successful tests would be required. Repetition of some tests on a planned basis is desirable for estimating confidence levels. Accordingly, the critical components should be capable of withstanding a minimum of 200 exposure tests, although cleaning of the optics may be required after fewer tests.

Section 2

DIVERTER AND TUBE DESIGN

2.1 PHYSICAL AND PRACTICAL CONSTRAINTS

a. Principal Limitations

The limiting constraints are imposed by the short focal length of the CNRS furnace and the need for containment of the peak flux to 450 cal/cm^2/sec at the bottom of a tube. Collimation of the total energy arriving at the focus is difficult with an economically acceptable optical configuration, and reducing the angular spread of the beam by using only a part of the furnace optical system would result in a reduction of the energy input.

Assuming a 250 cm^2 exposure sample, and a flux density of 450 cal/cm^2/sec, about 500 KW is required at the sample. This requires an optical system having an efficiency of 50 percent if all the solar input is used, and correspondingly higher if only a portion of the input is used. It is apparent that the optical system design should combine low loss reflecting or refracting surfaces with a wide angle of acceptance.

b. Durability

The requirement for about 200 exposures can be satisfied with components having inherent durability, by frequent replacement or refurbishing or a combination thereof. The need for highly efficient optical surfaces places a limitation on both approaches: good optical surfaces are expensive, and they may not be durable in a high flux density and dusty air flow environment. Since good collimation of the beam is unlikely, the containment tube interior will have to be reflective. The reflective surfaces will be subject to deterioration by the hot blow-off particles.

Cost imposes the real limitation. There is high confidence that a very efficient collimater and diverter could be designed, but its implementation would require expensive optical components and structural changes of the CNRS solar furnace. Hence, this design effort was directed toward a configuration which is self contained (i.e., which can be assembled and used in the furnace focal house without any significant modification to the furnace).

2.2 ALTERNATIVE APPROACHES

Previous studies of beam diversion have been conducted. The consideration of near horizontal soil, and integration into the White Sands Missile Range facility led to the conclusions that a diverting system with two refracting elements of unit magnification was preferred.[2] The overall scaled geometrics at WSMR are not very different than that at CNRS; however the increased power makes the WSMR preferred design of questionable use due to its power loss. In this study, SAI reviewed diversion techniques for the CNRS furnace. Five methods of diverting the beam were evaluated:

1. Plane mirrors
2. Parabolic concentration
3. Lenses
4. Light pipes
5. Ideal Light Collectors

Four criteria were used for evaluating each approach: compatibility with the furnace geometry, lowest costs, efficiency, and durability consistent with cost. As a result of the studies, a single design emerged that has the following general features. It is based on optical theory, and provides the maximum flux permitted for a given area. It is designed with minimum length reflecting elements for minimum power loss. It couples naturally into a confinement tube above the sample. The design of the flux diverter emerged after review of all five alternatives. The conclusions of the review were:

- <u>Plane Mirror</u>. Ruled out on compatibility and cost basis.
- <u>Parabolic Concentrator</u>. Ruled out on same basis.
- <u>Lenses</u>. Ruled out on cost and efficiency basis.
- <u>Light Pipes</u>. Ruled out on cost basis.
- <u>Ideal Light Collector</u>. Satisfactory.

A more detailed result of the preliminary review is given below.

a. Plane Mirror Diverter

The plane mirror alternative was quickly discarded. The verticle angle of the beam is 120^{o}, hence no configuration could capture all of the furance energy. Further, a reasonable separation between the mirror surface and the diverted focus is needed, which requires a very large mirror and places the focus in the inaccessible and inhospitable area within the furance beam and in front of the furance test house.

Figure 2-1 illustrates the problem imposed by a required 1.0 meter separation of focus and mirror surface, even if the verticality requirement is replaced by 15^{o}. The original focus, F_{o} is diverted to F_{D} by a mirror whose height is arbitrarily selected as 2 meters. This results in a loss of all energy from the vertical beam from an angle greater than $+ 30^{o}$ from the horizontal. To capture all of the energy in this reduced sector, the width of the mirror must be over 4M at the bottom and about 8.8M at the top. The diverted focus is then 1.7 meters out and .73 meters below the original focus, a point at which there is no existing structure.

b. Parabolic Concentrator

A parabola having its focus coincident with that of the furnace would, in theory, collimate the beam. However, the focal point of the furnace has finite size, and only the rays passing through the center would be collimated. By moving the focus of the parabola to a point beyond the furnace focus, a convergent effect of the parabola can be achieved. An attempt was made to define the geometry that would achieve the desired diversion (within 15^{o} of vertical) with acceptable loss of concentration. The baseline was predicated on an eccentricity of less than unity (an elipse) and having dimensions which are determined by the inter-focal distance. Such a surface would be very large and expensive to manufacture. Further consideration of the conic section was postponed pending evaluation of other alternatives.

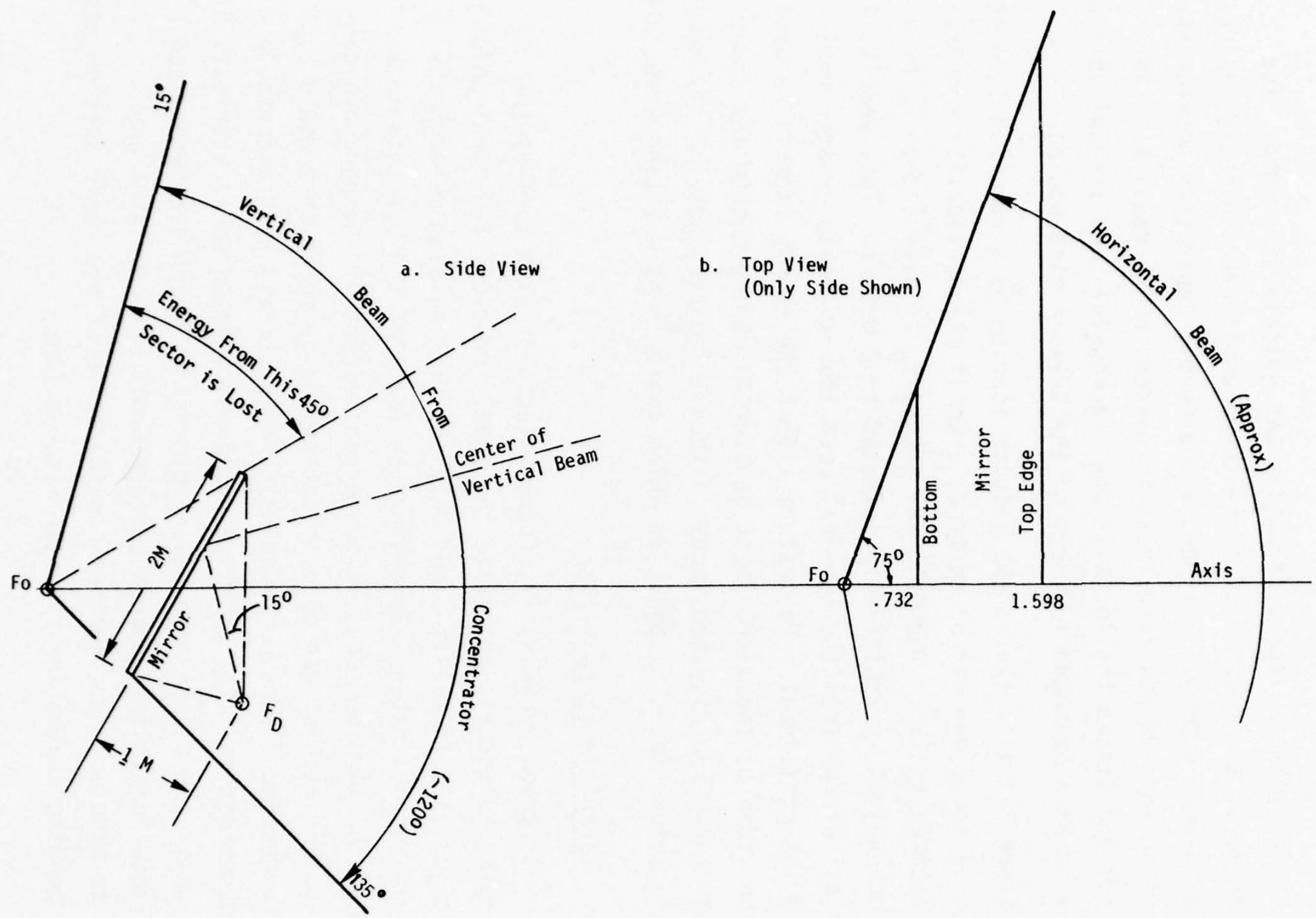

Figure 2-1. Plane Mirror Diverter

c. Lenses

An arrangement of lenses and a mirror similar to that used for diversion of the WSMR solar furnace beam is compatible with the geometry of the CNRS furnace (Reference 2).

The ratio of diameter to focal length of the collimating lens would be approximately 8:1. There are no stock lenses having such characteristics. A conventional lens would be excessively thick and therefore subject to large internal stresses from uneven heating. However, imaging quality is not important and a fresnel lens would be suitable. The one-time tooling costs for manufacture, and the uncertain durability in the CNRS furnace environment led to deferral of this approach pending the evaluation of other alternatives.

d. Light Pipes

Transparent rods or shapes, analogous to fiber optics, can efficiently transmit optical energy around controlled curvatures, hence a light pipe approach was investigated. The primary difficulty is the need to expose the input end of each pipe to rays having an angular spread within the internal trapping angle of the pipe material. This implies tapered inlet ends so that a "bees eye" configuration with each eye viewing a portion of the furnace concentrator, could intercept most of the energy.

A first order design indicated that the technique was feasible, but that each pipe element would be of a unique shape and that fabrication costs would be excessive. This approach was deemed less attractive from a cost aspect than the lens and mirror configuration.

e. Ideal Light Collector (ILC)

The conventional ILC does not divert optical energy into a desired direction, but its potential for concentration to offset reflection lossess led to an analysis of variations that might satisfy the requirements. A configuration was devised that appeared superior to the other alternatives, and effort was concentrated on refining the design. The configuration, termed, the "split" ILC, is described in paragraph 2.3 below.

2.3 DIVERTER OPTICAL DESIGN

2.3.1 Theory of the Ideal Light Collector (ILC)

A light collector is a device that accepts optical energy arriving over a range of finite angles, 2θ, and concentrates it to increase the flux density. It may be a 2- or 3-dimensional device.

To be termed "ideal", the collector must satisfy two criteria:

a. The concentration ratio (C_R) must equal the limit of Abbe's inequality which states for a 2-dimensional device:

$$C_R \leq \frac{1}{\mathrm{SIN}\Theta} .$$

This becomes $\frac{1}{\mathrm{SIN}^2\Theta}$ for a 3-dimensional device, and

b. It must have the minimum length, L, permissible by the usual relationship between aperture (D) and exit (d), that is

$$L = \frac{D + d}{2 \tan \Theta} .$$

$$\text{also } C_R \equiv \frac{D}{d}$$

In the mid-1960s Baranov and Mel'nikov in the U.S.S.R. and Hinterberger and Winston in the U.S. independently showed that the Abbe equality could be satisfied with a non-imaging specularly reflecting surface formed from a compound parabolic (Reference 3). Because the surfaces they defined provide the maximum concentration in minimum length, they are called Ideal Light Collectors.

The following example illustrates the geometric construction. An acceptance angle of 60^{o} (Θ=30) and an entrance plane diameter of unity are used. See Figure 2-2.

a. The entrance plane is drawn normal to the axis of symmetry of the collector (line ab = D)

b. Lines divergent from the axis of symmetry by the angle Θ are drawn from each side of the entrance plane (lines ae, bc)

c. Since the C_R for a two-dimensional figure is 2, i.e., $\frac{1}{\text{SIN } 30^{o}}$, then d (the exit plane length) must equal 1/2, and the length is $\frac{D+d}{2\tan\theta}$ = $\frac{1.5\sqrt{3}}{2}$, hence the exit plane (line ce) can be drawn.

d. The curved surface, a c, is a section of a parabola whose axis is paralleled to c b and whose focus is at point e. By computing the length of a e, and noting that it is at an angle of 2θ from the axis of parabola, the focal length can be derived and the parabola drawn. ae is equal to $\frac{D + d}{2 \text{ SIN } \Theta}$ = 1.5 and the focal length is then

$$\frac{(D + d)\ (1\text{-COS}2\theta)}{4 \text{ SIN}\Theta} = .375.$$

e. For a 3-dimensional collector, the line a c is rotated around the axis of symmetry to produce a surface of revolution. All rays crossing the entrance plane within the acceptance of 2Θ will pass through the exit plane. (It can also be shown that any ray entering the entrance plane at an angle $>\Theta$ with respect to the axis will ultimately be reflected back through the entrance plane.)

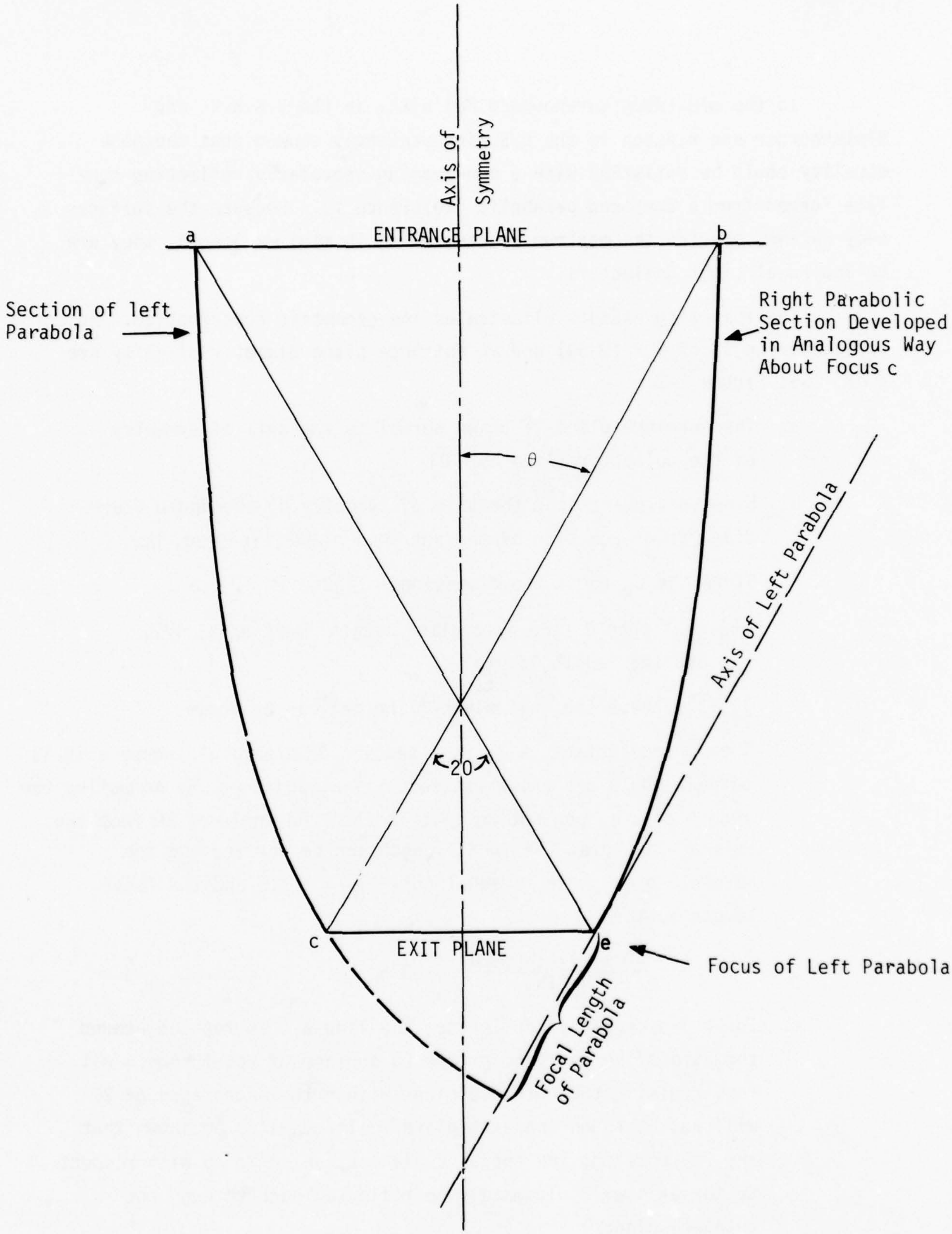

Figure 2-2. Ideal Light Collector Geometry

2.3.2 The "Split" ILC

To divert the beam into a vertical orientation without sacrificing the concentration attainable with the furnace geometry, a configuration called the "Split ILC" was devised. The split ILC was inspired by a design for a trough-type solar energy collector described by Winston (Reference 4).

The geometry of the cross section of Winston's trough-type collector is shown in Figure 2-3. All light entering the collector within the design acceptance angle strikes the fin. The fin is analogous to the exit plane. At first glance it seems that Abbe's equality has been violated because the length of the fin is only one-half that of the exit plane of an ILC of the type previously described. However, both sides of the fin must be included.

As a result of this work, it was noted that when one-half of the collector had the fin removed and a plane reflecting surface inserted along the axis from the entrance plane to the point where the fin was, the new device would have the same acceptance angle as previously but would now have an exit plane perpendicular to the entrance plane. The configuration is shown in Figure 2-4.

A split ILC is well suited to the application. By making the sides parallel, all entrant rays up to 90^{o} right or left of the axis will be trapped, and all rays within $\pm$ 60^{o} in the vertical can be redirected through the opening which was occupied by the fin in Figure 2-3. Physical construction is simple since no compound curved surface is involved.

An additional advantage accures from the slight concentration (1.16) achieved. Up to 16 percent of the input energy could be absorbed without a reduction in flux density at the output.

The geometric construction, assuming the entrance plane be be of unity height, is as follows (see Figure 2-3):

a) The line fd is normal to the exit plane and has a length equal to the ctn θ.
b) The segment acd is parabolic from a to c, and an arc from

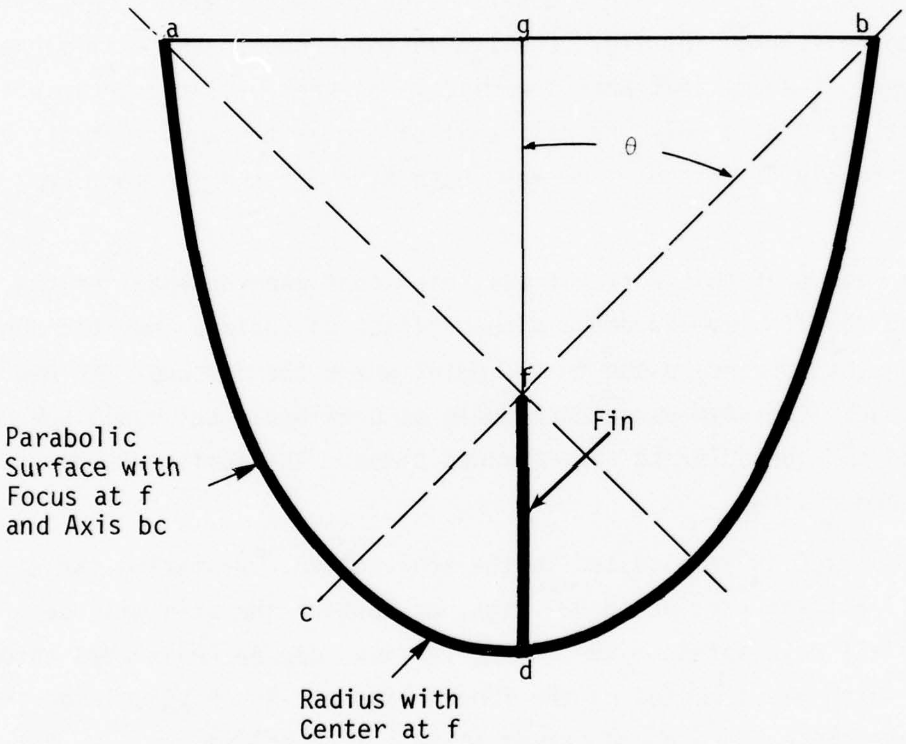

Figure 2-3. Geometry of ILC Variation

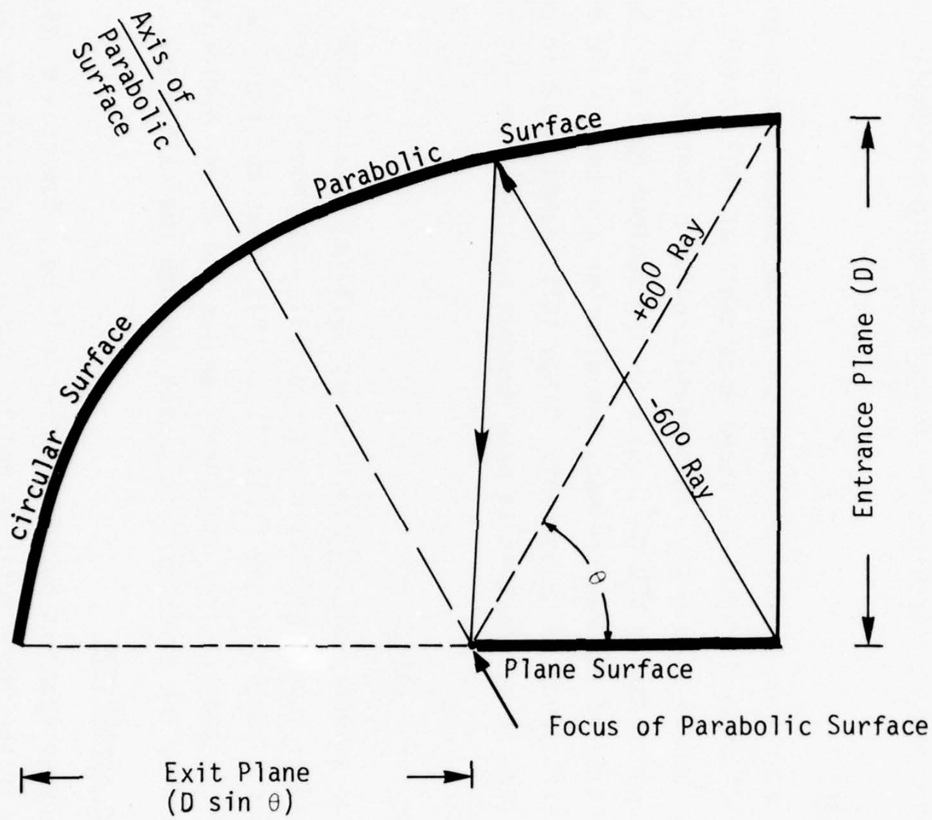

Figure 2-4. Geometry of Split ILC

c to d. The focus of the parabola and the center of the circle are at f, and the axis of the parabola contains bf. The radius of the circular portion is equal to the focal length of the parabola which is equal to $\sin\Theta$.

c) The height and width of the entry plane are chosen to include the half power contour in the furnace plane. Since that contour is approximately circular, the height and width are equal.

2.3.3 Ray Geometry

The first iteration for the diverter design was based upon an entrance plane 24 x 24 cm and a vertical acceptance angle of 120^o ($\Theta=60^o$). The exit plane is then 24 x 20.8 cm. This would provide a containment tube cross section of approximately 500 cm^2, which is the maximum desired. To achieve a flux density of 450 $cal/cm^2/sec$, the diverter and tube would require an optical efficiency of 82 percent. Since this seemed to be in the realm of possibility, it was decided to base further evaluation on the first design iteration.

a. Design verification

The ray geometry of the diverter was verified by a computer ray tracing program and by iconic simulation with a full scale model. Both methods confirmed the theory of the "split ILC." All light entering the entrance plane within the vertical acceptance angles and at any horizontal angle (up to 90^o) from the diverter axis passed through the exit plane.

b. Energy absorption

The energy absorbed by the diverter will be a function of the beam reflectivity of the inner surfaces and the number of reflections made by each ray. By a combination of graphic and analytical techniques, the number of reflections from the top and bottom surfaces for a ray entering at any vertical angle within the design limits is determined. For each elevation angle, a beam of parallel rays having a cross section exactly equal to a projection of the entrance plane is assured, and the average number of bounces per ray is determined. Figure 2-5 illustrates the method used and the results are shown in Figure 2-6. For all angles greater than 0^{o} and less than 60^{o}, some percentage of the rays pass directly through the exit plane without a top or bottom reflection. This results in the average number of reflections being less than unity in some cases.

Any ray entering the diverter can be contained in a plane elevated from the diverter axis by some angle θ and normal to the diverter sides, and upon reflection from the top or bottom, will enter a new plane which is also normal to the diverter sides.

The average length $(\bar{l})$ of the ray, projected onto the diverter sides, vs. elevation angle was determined by ray tracing. This average length was expressed as the ratio to width of the diverter $(\bar{l}/w)$. The number of side reflections is then $(\tan\theta)\ (\bar{l}/w)$, where θ is the horizontal angle, measured from the centerline, in the elevated plane.

To compute the energy absorption by the diverter, it was necessary to develop a projection of the furnace parabola onto a horizontal plane (equivalent to the heliostat field which provides essentially equal flux density onto a plane normal to the furnace axis). The intersections of vertically inclined planes originating at the focus and horizontal angles within those planes, with the parabola surface were then projected onto the plane. Finally the contours for the numbers of top and bottom reflections and side reflections were plotted. The results are shown in Figure 2- 7.

The contour values were integrated and the energy that would be absorbed by the diverter was calculated for several degrees of surface reflectivity. The results are shown in Figure 2-8. It is apparent that an efficient diverter is attainable without resort to very high quality (and fragile) optical surfaces, and that cooling of the diverter surfaces will not be necessary to produce the fluences required for the soil blow-off experiments.

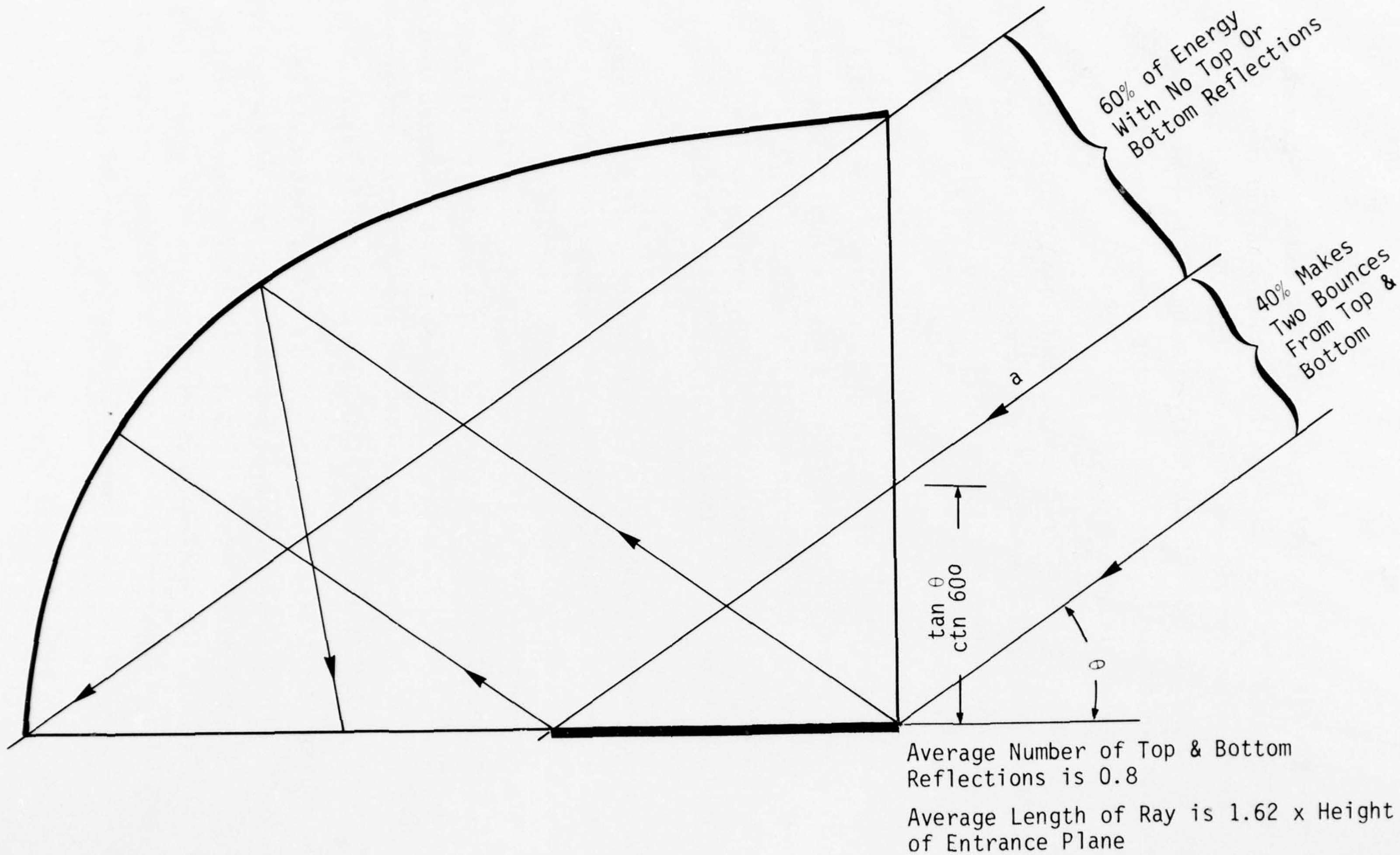

Figure 2-5. Example of Ray Tracing Method Used to Determine Number of Reflections vs. Elevation Angle (θ)

(1) $N = 2 \tan\theta \; ctn60^{o}$, $34.7^{o} \le \theta \le 60^{o}$

(2) $N = 1 + \tan\theta \; (ctn60^{o} - .75 csc60^{o})$ $13.9^{o} \le \theta \le 34.7^{o}$

(3) $N = 1.25 - .75 \tan\theta \; (csc60^{o} + ctn60^{o})$ $0^{o} \le \theta \le 13.9^{o}$

(4) $N = 1$, $-60^{o} \le \theta \le -36.6^{o}$

(5) A simple expression for N, $-36.6^{o} \le \theta \le 0$ is not apparent. Solution requires a 5 x 5 matrix.

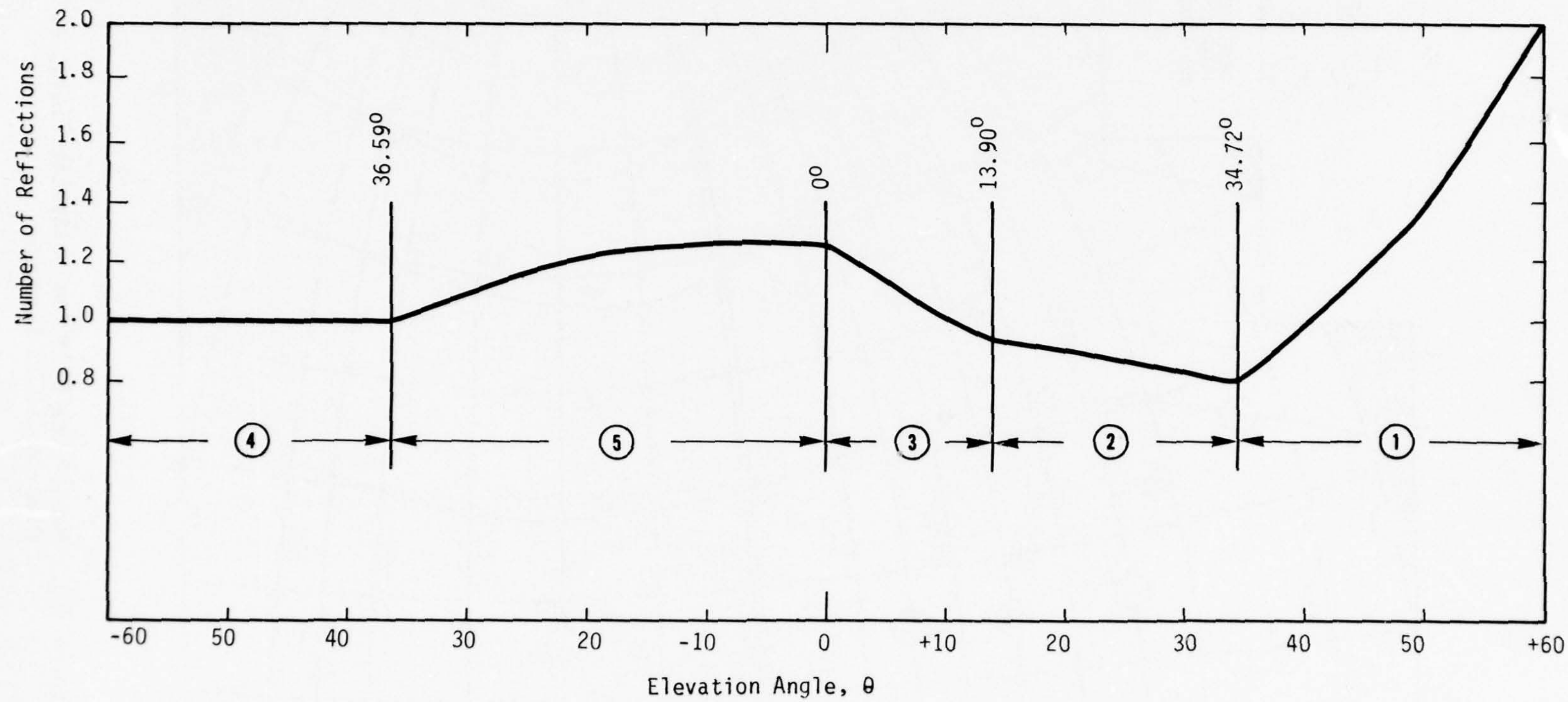

Figure 2-6. Number of Reflections from Top & Bottom Surfaces for Rays Entering in a Plane Tilted to θ

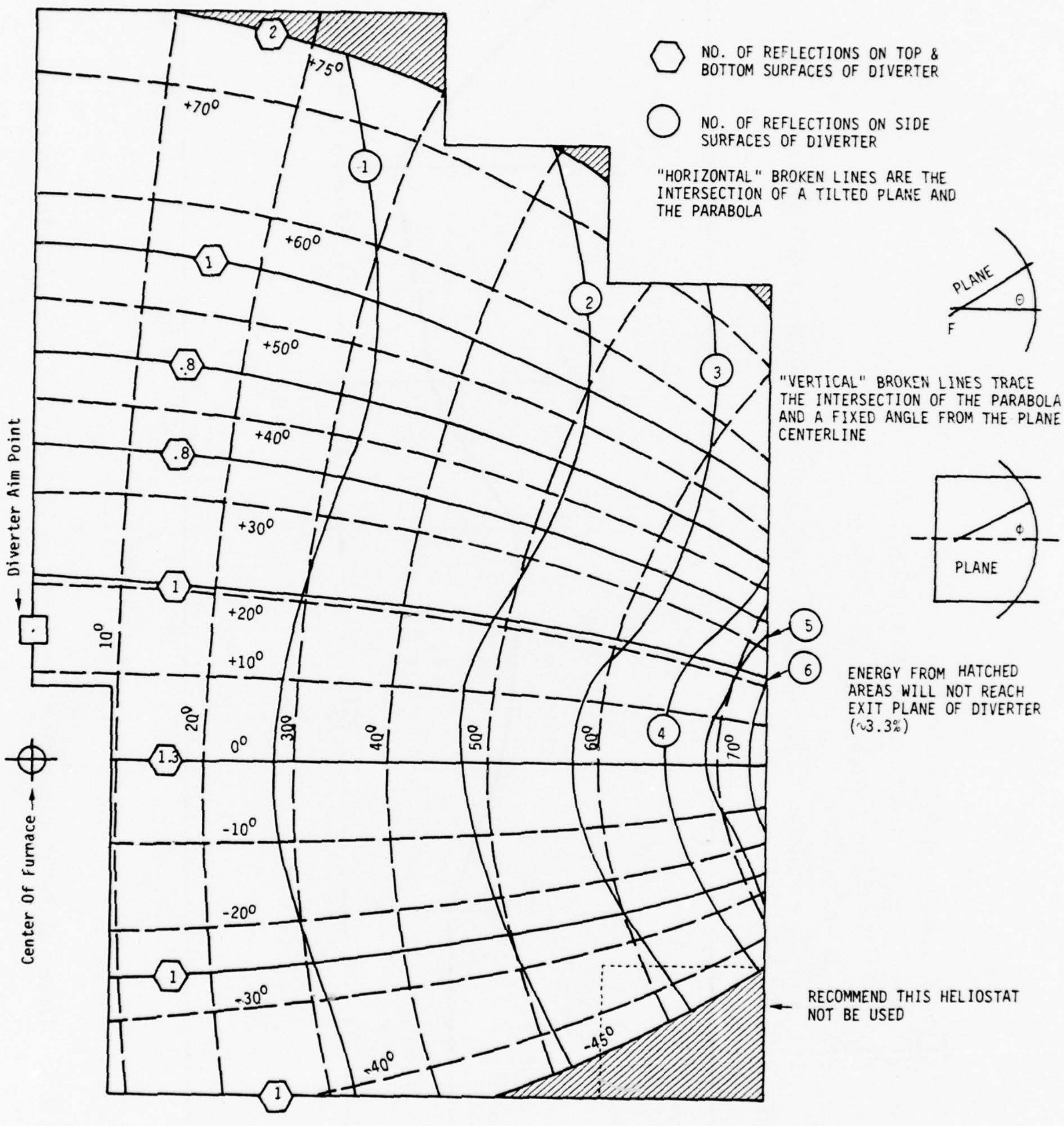

Figure 2-7. Map of One Half the Heliostat Field, as Projected onto the Diverter, CNRS Furnace

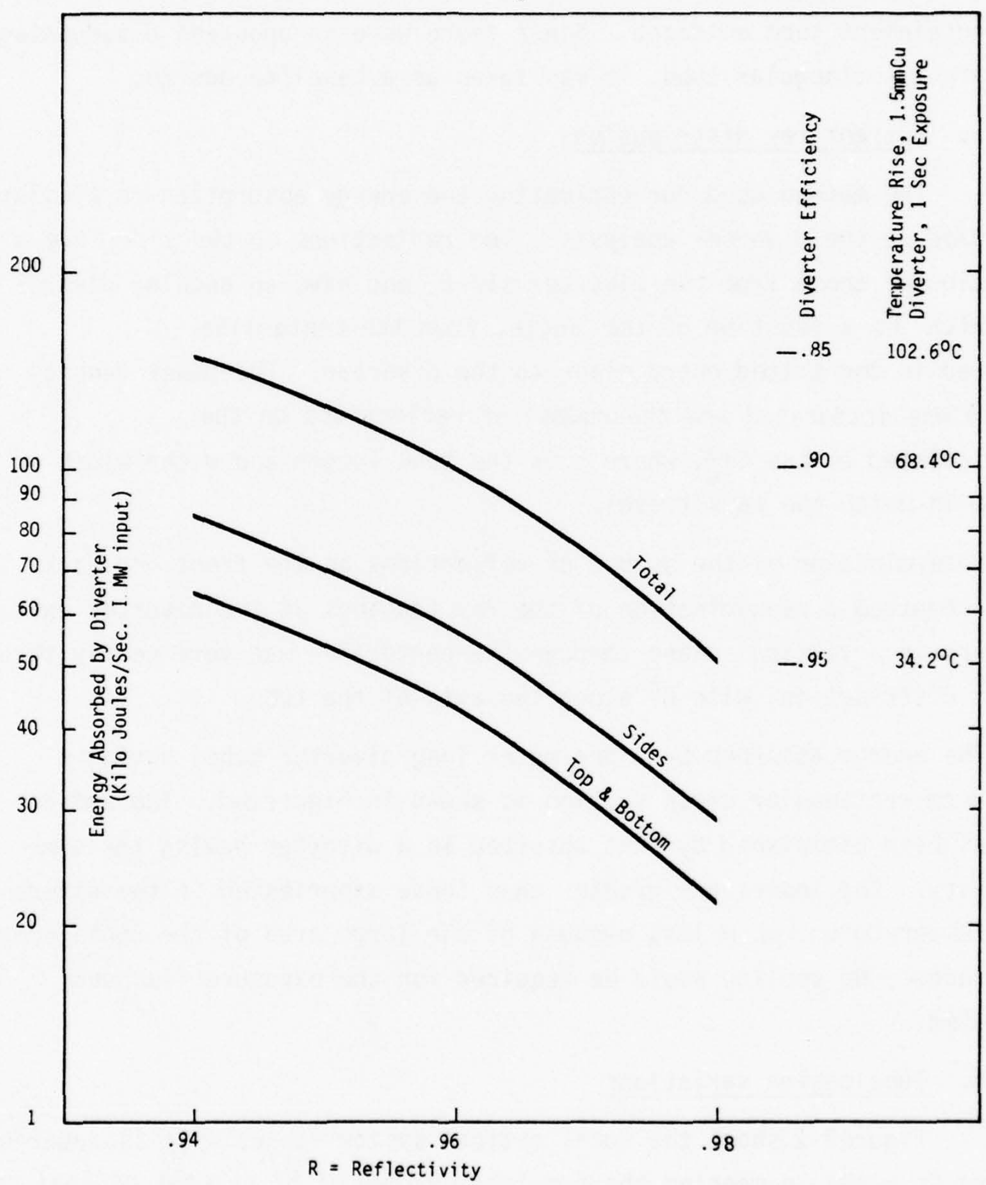

Figure 2-8. Energy Absorbed by the Diverter as a Function of Diverter Reflectivity

Section 3

CONTAINMENT TUBE DESIGN

The rectangular exit plane of the diverter dictates the cross section of the containment tube entrance. Since there were no apparent disadvantages to a straight rectangular tube, it was taken as a baseline design.

a. Entrant ray distribution

The method used for estimating the energy absorption is similar to that used in the diverter analysis. The reflections on the sides are a continuation of those from the diverter sides, and have an angular distribution which is a function of the angle, from the centerline, as measured in the tilted entry plane to the diverter. The power density vs. angle was integrated and the number of reflections on the sides calculated as $(\tan\theta)\frac{L}{w}$, where L is the tube length and w the width of the plane in which the rays travel.

Determination of the number of reflections on the front and back surfaces required a reexamination of the ray tracings at the diverter exit. The pattern in a vertical plane through the centerline was very nearly that of a $\cos^2$ distribution, with 0^o along the axis of the tube.

The energy absorbed by a one meter long diverter tube, having a 24 x 20.8 cm rectangular cross section is shown in Figure 3-1. The entrant energy has been diminished by that absorbed in a diverter having the same reflectivity. The losses are greater than those experienced in the diverter, but the temperature rise is less because of the large area of the containment tube surfaces. No cooling would be required for the exposure fluences contemplated.

b. Tube design variations

Figure 3-2 shows the total optical system losses. It is apparent the design is close to meeting the required minimum of 82 percent optical efficiency if suitable reflecting surfaces can be used. There is no apparent modification to the diverter that will further reduce losses. The simplest means for reducing losses is to shorten the containment tube (second curve on Figure 3-2).

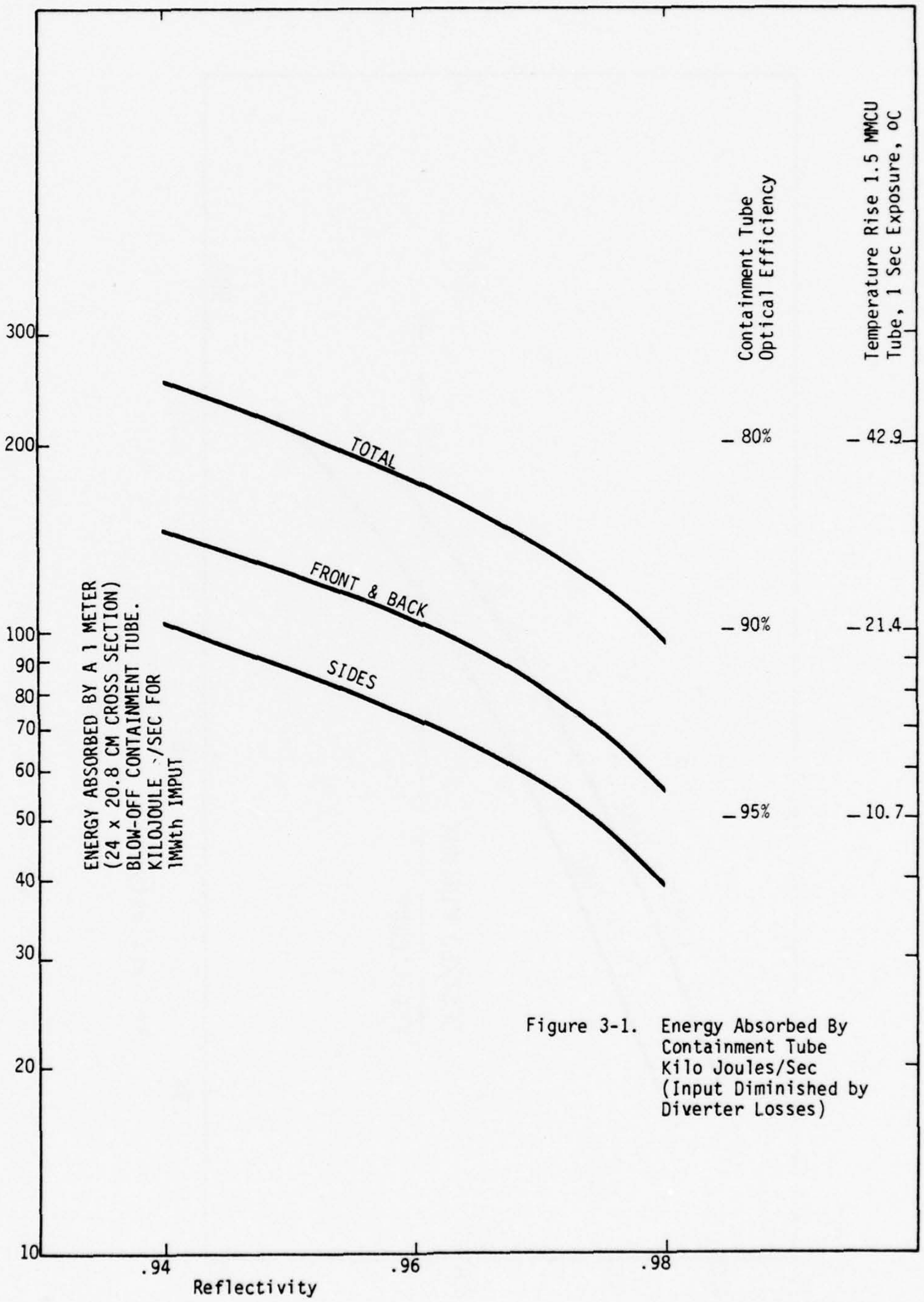

Figure 3-1. Energy Absorbed By Containment Tube Kilo Joules/Sec (Input Diminished by Diverter Losses)

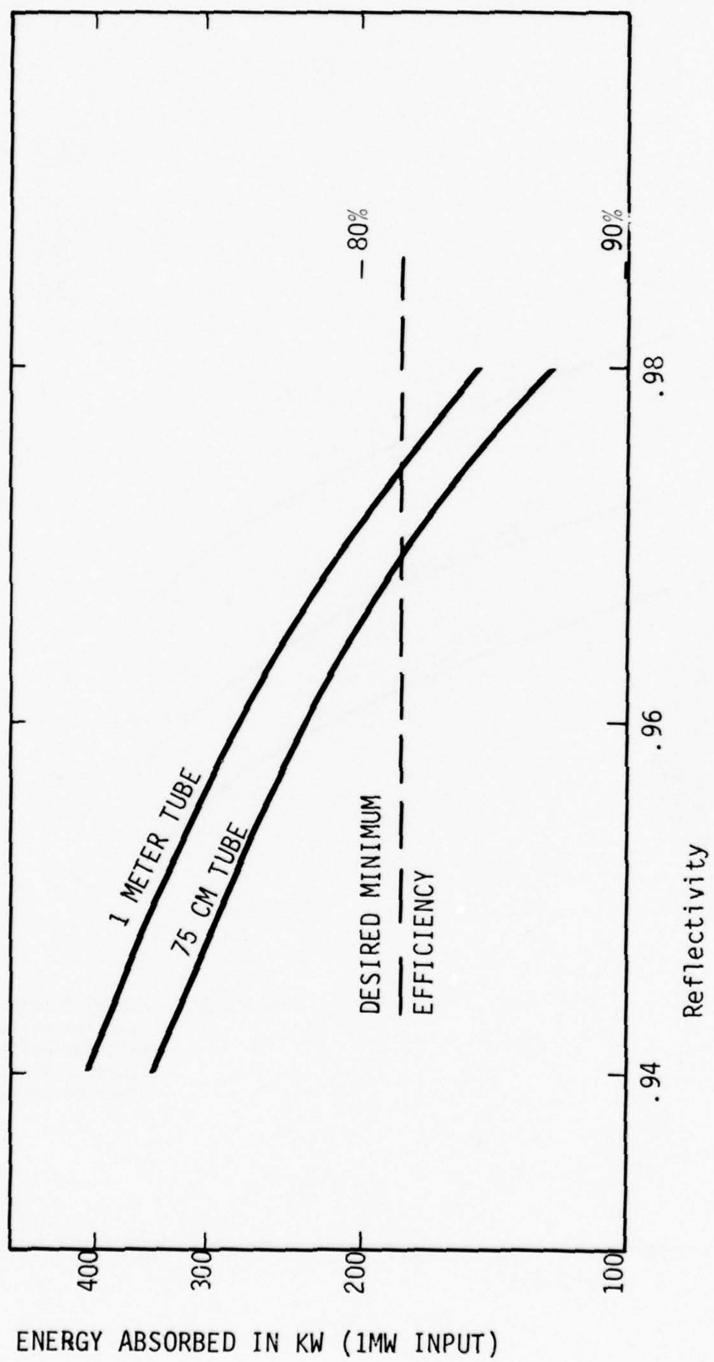

Figure 3-2. Total Optical System Losses

An ILC coupling the diverter exit to a reduced cross-section containment tube was considered, but the large dispersion angles at the diverter exit plane severely limit the gain that can be achieved, and the increase in tube losses (tube losses are proportioned to $\bar{1}/w$, and a reduced cross section would diminish w) more than offset any possible gain.

The opposite approach was considered, using an "inverted" ILC (its nominal exit plane being coupled to the diverter) to achieve a greater degree of collimation of the energy entering the containment tube. While this greatly reduces the reflection losses in the containment tube, the flux density loss from the increased area results in a net flux density loss at the bottom of the tube.

c. Instrument Aperture

The plane surfaces of the containment tube make instrument mounting simple. All instruments should be as small as practicable to minimize the size of the openings required, and all brackets should be on the exterior to prevent obscuration of the reflective surfaces. The losses resulting for apertures or obscuration of the reflecting surfaces will be about 225 watts per cm^2.

An aperture for photography represents the largest opening that would be required. Assuming a round opening of 4 cm dia, the losses would be slightly greater than 2.8 KW. Up to 14 small diameter (3mm) probes would eliminate only 1 cm^2 of reflective surface. It does not appear that aperture losses for a reasonable complement of instruments will amount to as much as one-half of one percent. More significant losses will result from blockage of the tube by the portion of the instrument which penetrates. The power density in the cross section will be about 1.7 KW per cm^2.

Section 4

TEST RESULTS

4.1 DIVERTER MODEL

The overall performance of an ideal light collector can easily be calculated. However, determining the energy distribution in the exit plane and the effects of fabrication tolerances would involve laborious calculations or extensive computer simulation. Accordingly, a full size model was constructed. The tolerances were those attainable with reasonable care, using standard shop tools. A pattern for the side plates was made on graph paper and transferred to plywood which was cut to shape with a bandsaw. The edges were sanded to smooth the curvature, and care was taken to adhere to the pattern. Polished aluminum plates were cemented to the surfaces and the upper and lower surfaces were fashioned from polished aluminum plate bent to conform to the edges of the plywood.

A translucent plastic plate with an inscribed graticule was placed over the exit plane, and the model was mounted in a tiltable stand with an inclination angle scale (it was much easier to tilt the model than to move the light source in elevation). The test set-up is illustrated in Figure 4-1.

A collimated light source was directed into the entrance plane and the position of the light beam plotted on the graticule as the elevation angle was varied. The tiltable mount was so constructed that the point of the light beam entry in the entrance plane could be adjusted, but would not change as a function of tilt angle. The elevation cut-off angles ($\pm 60^{\circ}$) were very sharp, and were exact within the limits of the elevation scale used (1° increments). The horizontal angle was controlled by moving the light source.

It was concluded that energy at this exit plane would have an approximately uniform distribution, and that the diverter performance was not sensitive to relatively crude fabrication tolerances.

A computer ray tracing model was also used to verify the performance of the iconic model. Equivalent conditions were simulated and the computer

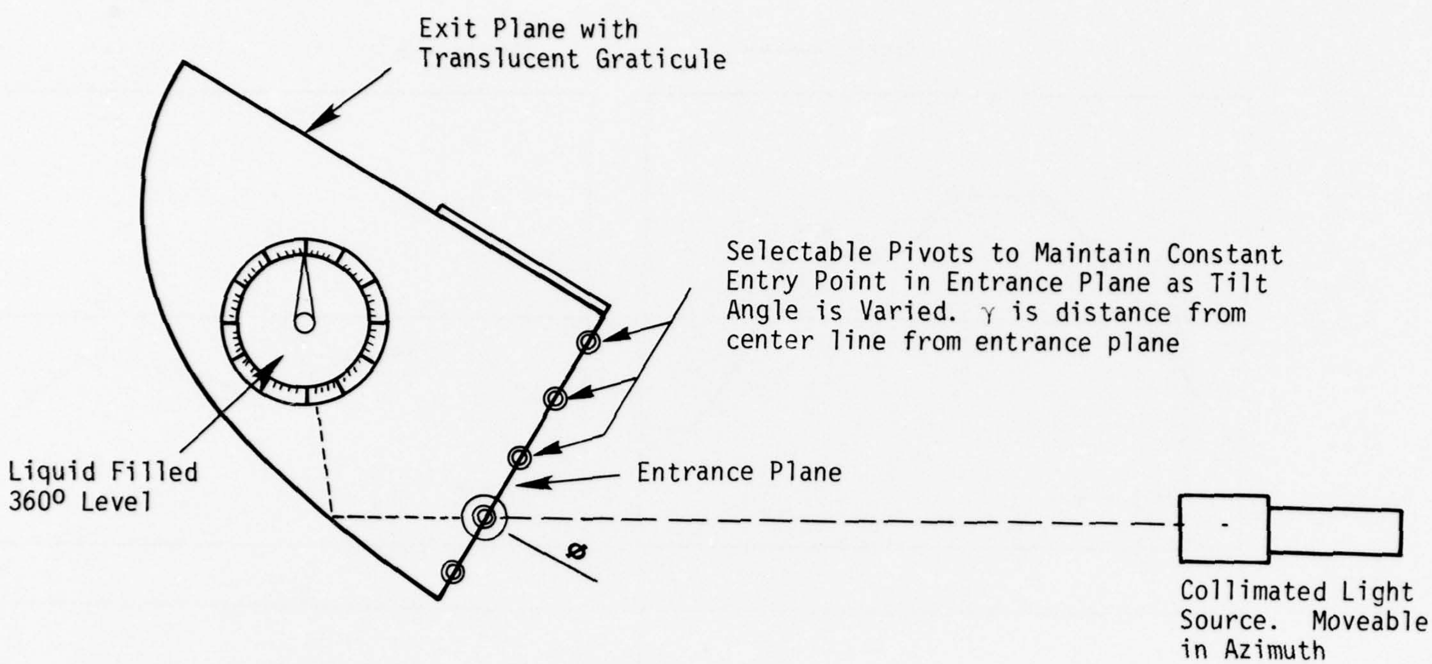

Note: Diverter Model was Mounted in an Inverted Position to Simplify Plotting

Figure 4-1. Diverter Model Test Set-Up

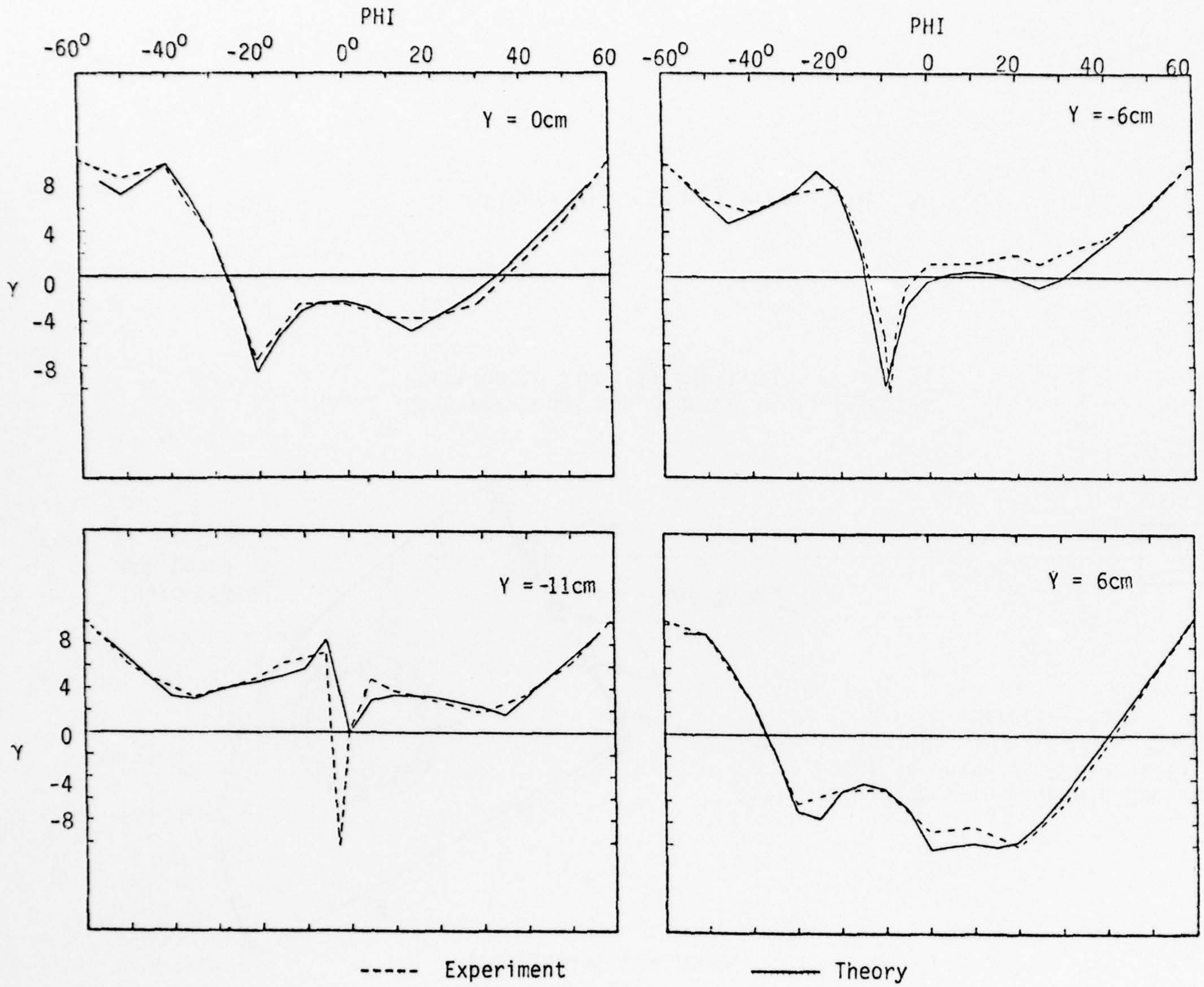

Figure 4-2. Comparison of Data with Theory CNRS Fullscale Model Diverter

data were overlaid on the plate taken from the graticule on the physical model. Figure 4-2 shows a comparison of representative data.

4.2 SURFACE REFLECTIVITY TESTS

a. Test method

The large number of reflections in the optical path from diverter entrance plane to soil sample makes the optical system performance sensitive to small changes in the reflectivity of the optical surfaces. Accordingly, the measurement of reflectivity must be made to tolerances of less than 1%.

To eliminate errors resulting from uncertainties in the intensity of the light source or the calibration of the detector, the set-up illustrated in Figure 4-3 was used. The test samples (two are required for each type of surface to be tested) are mounted in a parallel jaw holder which permits changing the distance between the sample faces. The detector is mounted in an integrating sphere and is operated in the photoconductive mode. A feedback amplifier was used to enhance linearity and to provide an output voltage range giving the greatest resolutions on a $4\frac{1}{2}$ digit DVM.

The dark current (converted to voltage and amplified) was recorded prior to each test. The mirror holder was operated to provide for 0, 2, 4, etc. reflections, and the reading for each was recorded. After the dark voltage was subtracted, the logarithm of the detector voltage was plotted as a function of the number of reflections.

The foregoing method eliminates all errors and uncertainties except those due to noise and nonlinear response of the detector and the voltmeter. By using the photoconductive mode and a feedback amplifier. the nonlinearity errors are minimized. They were checked, and transmission tests verified that they were small. The confidence can be estimated by the conformance of the plotted data to a straight line. Also absolute value errors of the calculated reflectivity are estimated to be less than $\pm$ 0.4%.

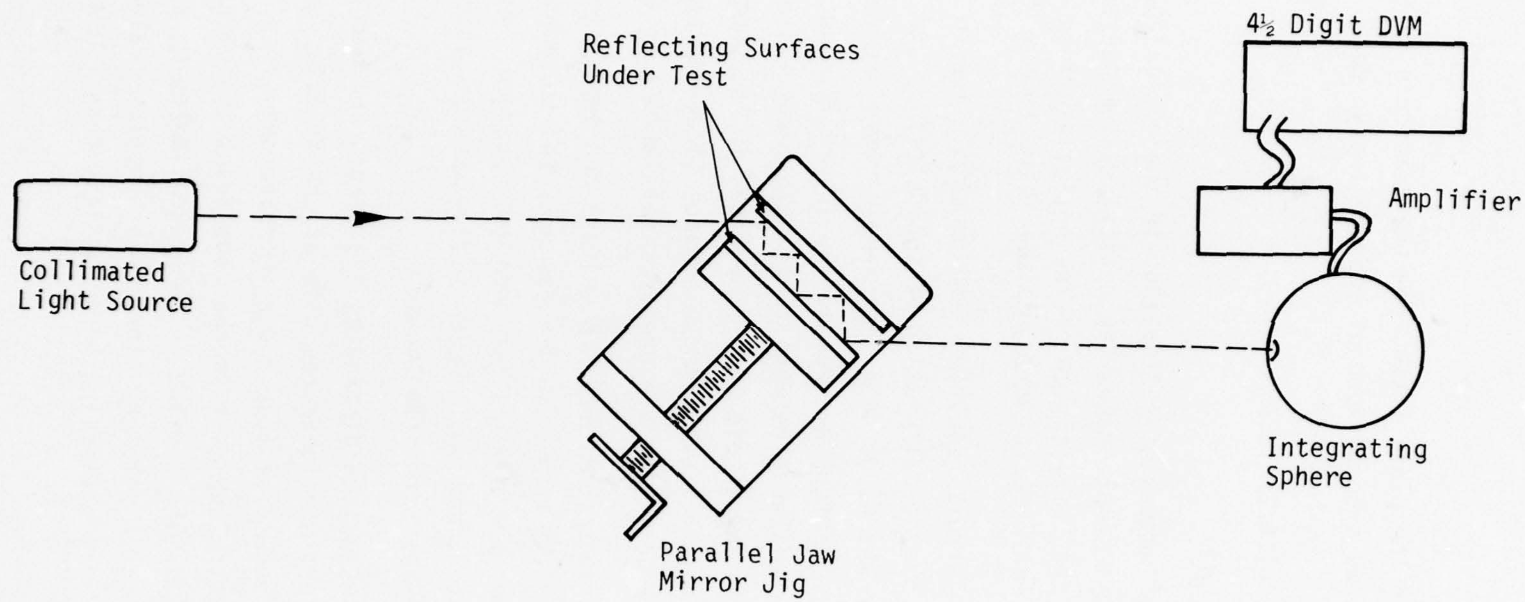

Figure 4-3. Reflectivity Measurement Set-Up

Figure 4-4 shows several data plots. The reflectivity, R, is

$$R = \sqrt[M-N]{\frac{\text{Voltage at M+N Reflections}}{\text{Voltage at N Reflections}}}$$

where M&N are the number of reflections for which output data exists

b. Test data

The least expensive "good" quality surface is vacuum deposited aluminum. Several samples were measured with uniform results. Reflectivities of 0.870 with white light (tungsten source), 0.864 with yellow (YI filter and a tungsten source) and 0.858 with Red (HeNe laser) were measured. Subsequent design data showed that much better reflectivities would be needed, hence no further tests of aluminum surfaces were made.

Several samples of vacuum deposited silver with a silicon oxide protective coating were tested. While the manufacturers' data show these to have a reflectivity of 0.99 from about .35μ to well into the infrared, all tests showed them to be in the range of 0.972 to 0.98. This is adequate for the optical system requirements, but the surfaces are relatively fragile.

Two samples of heavily silver-plated brass were obtained. The brass was first polished, then a one-half mil nickel plating applied, followed by a one-mil silver plating which was polished to commercial silver plate ("color polish") standards. The plating was heavy enough to permit repeated repolishing, and it was anticipated that this would provide an acceptable surface for the containment tube. Reflectivity of the plates, as received, was .931 and was independent of light color.

These were not true mirror surfaces, and while they preserved a definable image of the light spot even after 12 to 16 reflections, a halo of scattered light could be observed around the spot. The dynamic range of the detector was inadequate to measure this halo. Since this was clearly forward scattering (divergence from the point of first reflection was about 5 to 6^{o}), the actual performance will be better than that measured.

The surfaces were repolished numerous times using different polishes and polishing techniques. The best of these (a commercial silver polish applied with cheese cloth in a circular motion) provided a reflectivity

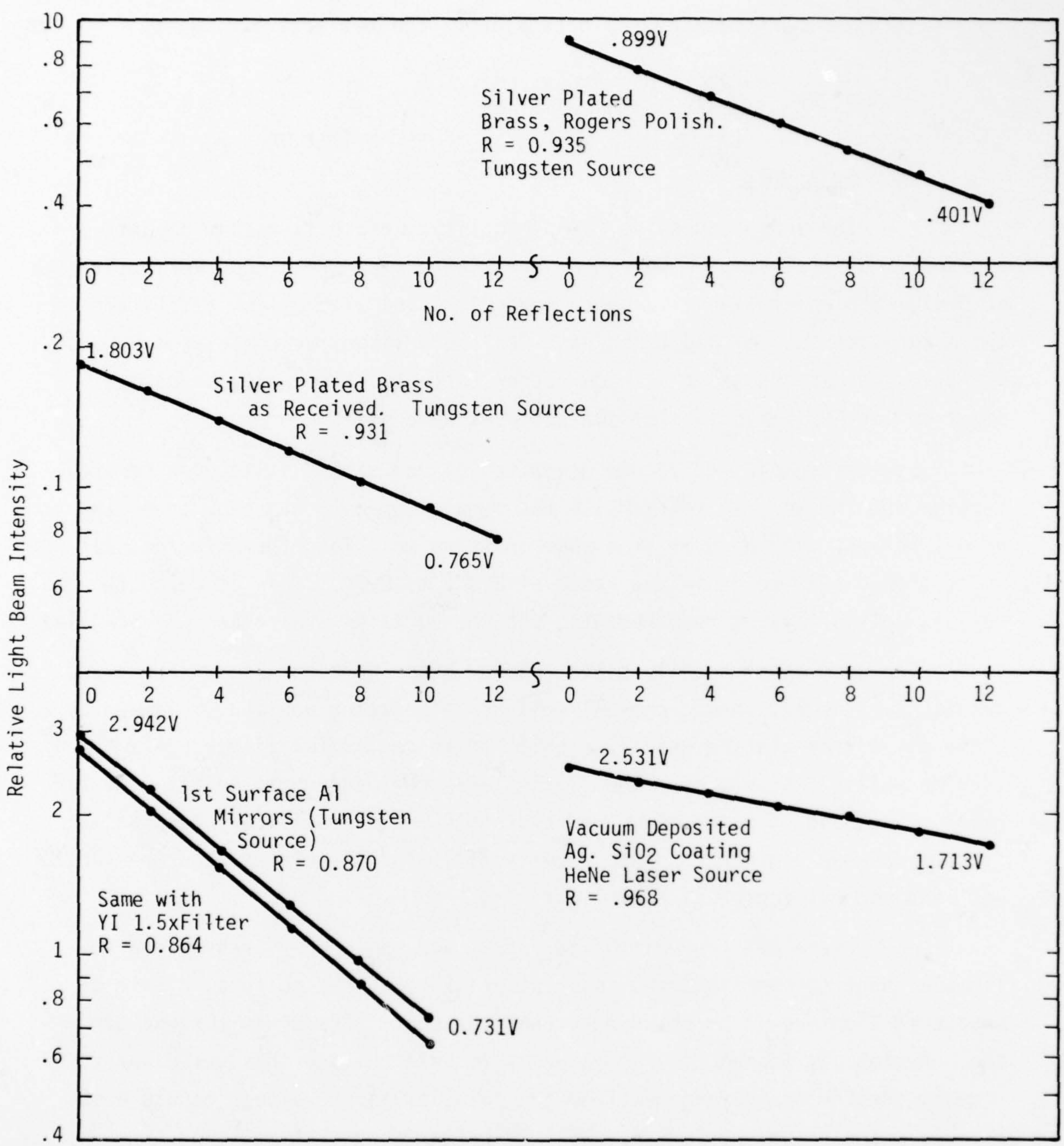

Figure 4-4. Typical Reflectivity Data

slightly better than the original polish (.935). This small difference, if it is indeed real, may be due to tarnish. The original surfaces were measured several days after manufacture while the repolished surface was measured within an hour.

The heavy silver plate is a rugged surface that would withstand the containment tube environment for multiple exposures with occasional re-polishing, and has adequate reflectivity.

Section 5

IMPLEMENTATION

5.1 GENERAL

The limited scope of the project has resulted in a geometrical design for an optical system and the development of accurate data on several candidate reflective coatings. This section enumerates the subsequent steps that will be necessary before plans and schedules for a soil blow-off test series using the CNRS solar furnace can be finalized.

5.2 OPTICAL SYSTEM IN-SITU TESTS

The highest priority item for continuation of the program is the construction and testing of the optical systems. This is needed to finalize the design, to determine the number of components required for completion of a test program, and to accurately estimate the on-site time that will be required.

To meet the requirements for 450 cal/cm^2/sec peak at the soil sample, it is apparent that some compromises will be required in the design postulated in the foregoing sections. Two of the surfaces tested, the vacuum deposited silver and the heavy silver plate have been considered as candidates. The former is the most reflective but is relatively fragile, the latter is rugged, but rather lossy. Another variable is the length of containment tube. One meter was selected as an initial point, and is certainly adequate, if not excessive. If a shorter tube is satisfactory, the requirements on the optical surfaces may be relaxed somewhat.

Since the containment tube is subject to damage from blow-off particles, the plated silver is the most appropriate finish. The diverter will be subjected to less damage from hot particles and the vacuum deposited coating may be suitable.

Table 5-1 summarizes the optical efficiences attainable for different combinations of tube lengths and reflective coatings. All that meet the

Table 5-1. Optical Efficiencies For Several Design Combinations

CONTAINMENT TUBE		DIVERTER REFLECTIVE COATING	
Reflective Coating	Length	Heavy Silver Plate	Vacuum Deposited Silver
Heavy Silver Plate	1 M	62%	69%
	75 cm	68%	76%
	50 cm	74%	82%
Vacuum Deposited Silver	1 M		85%
	75 cm		88%
	50 cm		90%

82 percent minimum efficiency requirement use vacuum deposited silver on the diverter surfaces. Only the 50 cm containment tube length permits meeting the 82 percent requirement with heavy silver plate.

The optical system test program should provide for testing the two combinations, both of which use diverters with vacuum deposited silver. One should have a 50 cm silver plated containment tube and the other a one-meter vacuum deposited tube. The tests should measure their optical efficiency and their resistance to damage from blow-off particles.

5.3 INSTRUMENT SELECTION AND INTEGRATION

The data requirements identified in Section 1 can be satisfied with relatively simple instruments, but their precise dimensions, placement, and manner of attachment must be determined before the optical component shop drawings can be completed.

Aspirated thermocouples are the recommended choice for air temperature measurements within the containment tube. Small size (1/8" dia) units have been successfully used in other solar furnace tests (Reference 5). These will not diminish the reflecting areas of the tube significantly, but their total cross section will intercept appreciable energy. For example, 5-1/8" tubes each extending to the center of the tube from either the front or back would intercept about 26 KW. Since their surfaces will be reflective, they will absorb very little energy, but about one-half of it will be diffusely scattered back toward the entrance plane.

The problems associated with high speed photography of events within the tube have not been addressed in detail. An aperture sufficient for photography will not have a significant effect on optical losses. If the camera is aimed slightly downward there should be little risk of high intensity light being reflected into the camera lens. However, a means for providing a contrasting background without adverse impact on optical efficiency is not readily apparent. It is recommended that the initial tests of the optical components include time and resources for photography experiments.

REFERENCES

1. F. Trombe, et al., "The French CNRS 1000 kw Solar Furnace Description, Performance Characteristics and Present Utilizations and Perspectives," presented at the NFS International Seminar on Large Scale Solar Energy Test Facilities, November 18 to 19, 1974, New Mexico State University, Las Cruces, New Mexico.

2. T. M. Knasel, "Thermal Induced Blow-Off - A Report on Experimental Studies," Volume I and II, DNA 3723F-1 and -2, 15 April 1975.

3. V. K. Baranow and G. K. Mel'nikov,"Study of the Illumination Characteristics of Hollow Focons," Soviet Journal of Optical Technology, Volume 33, #5, page 408, September 1966.

   H. Hinterberger and R. Winston, "Efficient Light Coupler for Threshold Cerenkov Counters," The Review of Scientific Instruments, Vol.37, #8, page 1094, August 1966.

4. R. Winston and H. Hinterberger, "Principals of Cylindrical Concentrators for Solar Energy," Solar Energy, Vol. 17, page 225, 1975.

5. T. M. Knasel, "Experimental Studies of Soil Thermal Irradiation," *Volume I, Soil Blow-Off Data Analysis, DNA 4484-1, Table 12, page 68,* 15 April 1977.

PRECEDING PAGE BLANK - not FILMED

DISTRIBUTION LIST

DEPARTMENT OF DEFENSE

Assistant to the Secretary of Defense
Atomic Energy
ATTN: Honorable Donald R. Cotter

Director
Defense Advanced Rsch. Proj. Agency
ATTN: Technical Library
ATTN: NMRO
ATTN: PMO
ATTN: STO

Director
Defense Civil Preparedness Agency
Assistant Director for Research
ATTN: Admin. Officer

Defense Documentation Center
Cameron Station
12 cy ATTN: TC

Director
Defense Intelligence Agency
ATTN: DB-4C, Edward O'Farrell
ATTN: DT-1C
ATTN: DT-2, Wpns. & Sys. Div.

Director
Defense Nuclear Agency
ATTN: TISI, Archives
ATTN: DDST
2 cy ATTN: SPSS
3 cy ATTN: TITL, Tech. Library

Chairman
Dept. of Defense Explo. Safety Board
ATTN: DD/S&SS
ATTN: Thomas Zaker

Commander
Field Command, DNA
ATTN: FCPR
ATTN: FCT
ATTN: FCTMOF

Chief
Livermore Division, Fld. Command, DNA
Lawrence Livermore Laboratory
ATTN: FCPRL

Commandant
NATO School (SHAPE)
ATTN: U.S. Documents Officer

Chief
Test Construction Division
Field Command Test Directorate
ATTN: FCTC

Under Secretary of Def. for Rsch. & Engrg.
Department of Defense
ATTN: AE
ATTN: S&SS (OS)

DEPARTMENT OF THE ARMY

Dep. Chief of Staff for Rsch. Dev. & Acq.
ATTN: Technical Library

Chief of Engineers
ATTN: DAEN-MCE-D
ATTN: DAEN-RDM

Deputy Chief of Staff for Ops. & Plans
ATTN: Technical Library

Commander
Harry Diamond Laboratories
ATTN: DELHD-NP
ATTN: DELHD-TI, Tech. Lib.

Commander
Redstone Scientific Information Ctr.
U.S. Army Missile Command
ATTN: Chief, Documents

Director
U.S. Army Ballistic Research Labs.
ATTN: J. H. Keefer, DRDAR-BLE
ATTN: Julius J. Meszaros, DRXBR-X
ATTN: Tech. Lib. Edward Baicy
ATTN: W. Taylor, DRDAR-BLE

Director U.S. Army Engr. Waterways Exper. Sta.
ATTN: Guy Jackson
ATTN: John N. Strange
ATTN: Technical Library
ATTN: William Flathau

Commander
U.S. Army Mat. & Mechanics Rsch. Ctr.
ATTN: Technical Library

Commander
U.S. Army Materiel Dev. & Readiness Cmd.
ATTN: Technical Library

Commander
U.S. Army Mobility Equip. R&D Ctr.
ATTN: Technical Library

Commander
U.S. Army Nuclear & Chemical Agency
ATTN: Library

DEPARTMENT OF THE NAVY

Chief of Naval Material
ATTN: MAT 0323

Chief of Naval Operations
ATTN: OP 981
ATTN: OP 03EG

Commander
David W. Taylor Naval Ship R&D Ctr.
ATTN: Code L42-3, Library

DEPARTMENT OF THE NAVY (Continued)

Chief of Naval Research
ATTN: Code 461, Jacob L. Warner
ATTN: Code 464, Thomas P. Quinn
ATTN: Nicholas Perrone
ATTN: Technical Library

Officer-in-Charge
Civil Engineering Laboratory
Naval Construction Battalion Center
ATTN: R. J. Odello
ATTN: Technical Library

Commander
Naval Electronic Systems Command
Naval Electronic Systems Cmd. Hqs.
ATTN: PME 117-21A

Commander Naval Facilities Engineering Command
Headquarters
ATTN: Code 03A
ATTN: Technical Library
ATTN: Code 04B

Director
Naval Research Laboratory
ATTN: Code 2600, Tech. Lib.

Commander
Naval Sea Systems Command
ATTN: ORD-91313, Library
ATTN: Code 03511

Commander
Naval Ship Engineering Center
ATTN: NSEC 6105G
ATTN: Technical Library

Officer-in-Charge
Naval Surface Weapons Center
ATTN: Code WA501, Navy Nuc. Prgms. Off.

Commander
Naval Surface Weapons Center
Dahlgren Laboratory
ATTN: Technical Library

Director Strategic Systems Project Office
ATTN: NSP-272
ATTN: NSP-43, Tech. Lib.

DEPARTMENT OF THE AIR FORCE

AF Geophysics Laboratory, AFSC
ATTN: LWW, Ker C. Thompson

AF Institute of Technology, AU
ATTN: Library, AFIT Bldg. 640, Area B

AF Weapons Laboratory, AFSC
ATTN: DES-S, Maj Ganong
ATTN: DES-C, Charles Needham
ATTN: SUL
ATTN: DEX

Headquarters, Air Force Systems Command
ATTN: DLCAW

Hq. USAF/IN
ATTN: INATA

DEPARTMENT OF THE AIR FORCE (Continued)

Hq. USAF/RD
ATTN: RDQSM

Commander in Chief
Strategic Air Command
ATTN: NRI-STINFO, Library

DEPARTMENT OF ENERGY

Albuquerque Operations Office
ATTN: Doc. Con. for Tech. Library

Division of Headquarters Services
Library Branch G-043
ATTN: Doc. Con. for Class. Tech. Lib.

Nevada Operations Office
ATTN: Doc. Con. for Tech. Lib.

Division of Military Application
ATTN: Doc. Con. for Test Office

University of California
Lawrence Livermore Laboratory
ATTN: Larry W. Woodruff, L-96
ATTN: Tech. Info. Dept. L-3

Los Alamos Scientific Laboratory
ATTN: Doc. Con. for Reports Lib.

Sandia Laboratories
Livermore Laboratory
ATTN: Doc. Con. for Tech. Lib.

Sandia Laboratories
ATTN: Doc. Con. for Org. 3422-1,
Sandia Rpt. Coll.

DEPARTMENT OF DEFENSE CONTRACTORS

Aerospace Corporation
ATTN: Tech. Info. Services

The Boeing Company
ATTN: Aerospace Library

Civil/Nuclear Systems Corp.
ATTN: Robert Crawford

EG&G Washington Analytical Services Center, Inc.
ATTN: Technical Library

General Electric Company
TEMPO-Center for Advanced Studies
ATTN: DASIAC

IIT Research Institute
ATTN: Technical Library

Institute for Defense Analyses
ATTN: IDA Librarian, Ruth S. Smith

Kaman Sciences Corporation
ATTN: Library

Lockheed Missiles & Space Co., Inc.
ATTN: Technical Library

DEPARTMENT OF DEFENSE CONTRACTORS (Continued)

Physics International Company
ATTN: Doc. Con. for Coye Vincent
ATTN: Doc. Con. for E. T. Moore
ATTN: Doc. Con. for Tech. Lib.

R&D Associates
ATTN: J. G. Lewis
ATTN: Technical Library
ATTN: Robert Port

Science Applications, Inc.
ATTN: Technical Library

Science Applications, Inc.
ATTN: R. A. Shunk

Science Applications, Inc.
ATTN: J. Dishon

Science Applications, Inc.
ATTN: T. M. Knasel
ATTN: J. Cockayne
ATTN: A. Houghton

Southwest Research Institute
ATTN: A. B. Wenzel
ATTN: Wilfred E. Baker

SRI International
ATTN: George R. Abrahamson
ATTN: Burt R. Gasten

DEPARTMENT OF DEFENSE CONTRACTORS (Continued)

Systems, Scinece and Software, Inc.
ATTN: Donald R. Grine
ATTN: Technical Library

TRW Defense & Space Sys. Group
2 cy ATTN: Peter K. Dai, R1-2170
ATTN: Tech. Info. Center, S-1930
ATTN: D. H. Baer, R1-2136

TRW Defense & Space Sys. Group
San Bernardino Operations
ATTN: E. Y. Wong, 527-712

The Eric H. Wang
Civil Engineering Rsch. Fac.
The University of New Mexico
ATTN: Larry Bickle
ATTN: Neal Baum

Weidlinger Assoc. Consulting Engineers
ATTN: Melvin L. Baron

Weidlinger Assoc. Consulting Engineers
ATTN: J. Isenberg

IED

-78